Active-to-passive oxidation transition for polycarbosilane-derived silicon carbide fibers heated in Ar-O₂ gas mixtures

T. SHIMOO, K. OKAMURA
Department of Metallurgy and Materials Science, Graduate School of Engineering,
Osaka Prefecture University, 1-1, Gakuen-cho, Sakai, 599-8531 Osaka, Japan
E-mail: shimoo@mtl.osakafu-u.ac.jp

Y. MORISADA
Osaka Prefecture University, 1-1, Gakuen-cho, Sakai, 599-8531 Osaka, Japan

The active-to-passive oxidation transition for three types of polycarbosilane-derived SiC fibers (Nicalon, Hi-Nicalon and Hi-Nicalon S) was examined at 1773 K through TG, XRD analysis, SEM observation and tensile tests. The oxygen partial pressure for the active-to-passive oxidation transition decreased in the following order: $p_{O_2} = 100$–250 Pa for Nicalon, $p_{O_2} = 10$–25 Pa for Hi-Nicalon and $p_{O_2} = 1$–2.5 Pa for Hi-Nicalon S. Considerable strength was retained in the passive-oxidation region. The active-oxidation produced a marked decrease in strength of Nicalon and Hi-Nicalon ($\sigma \fallingdotseq 0$ GPa). On the other hand, the strength of Hi-Nicalon S after active-oxidation was nearly identical to that after passive-oxidation ($\sigma \fallingdotseq 1$ GPa). © *2002 Kluwer Academic Publishers*

1. Introduction

The oxidation of bulk SiC has been extensively studied in various oxidizing environments. The oxygen partial pressure of oxidizing environments is an important factor controlling the oxidation-resistance of SiC. Under high and moderate oxygen partial pressures, SiC is passively oxidized and the resulting stable silica film protects the material from further oxidation. On the other hand, under low oxygen partial pressures, SiC is subjected to active-oxidation accompanied by the formation of gaseous products, resulting in serious damage to SiC. Thus, the passive-to-active oxidation transition is a critical factor influencing the morphologies, microstructure and mechanical properties of SiC after an oxidation test. Therefore, the active-to-passive oxidation transition in CVD-SiC and sintered SiC has been theoretically and experimentally investigated in detail by many researchers [1–12].

Polycarbosilane-derived SiC fibers such as Nicalon, Hi-Nicalon and Hi-Nicalon S (Nippon Carbon Co., Tokyo, Japan) are employed as reinforcing material in ceramic-matrix composites for high-temperature applications in oxidizing atmospheres. The oxidation behavior of fibers seems to be greatly different from that of bulk SiC, owing to the existence of an amorphous silicon oxycarbide phase and/or free carbon. Many investigations have been carried out for the passive-oxidation of SiC fibers in oxidizing atmosphere with high oxygen partial pressures, such as air, H_2-H_2O, O_2 and Ar-O_2 gas mixtures [13–30]. However, very little work has been made on the active-oxidation of SiC fibers [19]. In a previous report, the present authors studied the oxidation behavior of Nicalon at 1773 K in Ar-O_2 gas mixtures with oxygen partial pressures from 100 to 100000 Pa [31]. The active-to-passive transition was found between oxygen partial pressures of 100–250 Pa. While the fiber strength was considerably retained in the passive-oxidation region, it was lost in the active-oxidation region. It is anticipated that there might be a large difference in the oxidation behavior between the three types of SiC fibers, owing to their different compositions and microstructures. In the present work, the oxidation behaviors of Hi-Nicalon and Hi-Nicalon S at 1773 K under oxygen partial pressures of 1–25000 Pa were investigated through thermogravimetry experiments, X-ray diffraction analysis, scanning electron microscopic observation and tensile tests. The oxygen partial pressures for the active-to-passive oxidation transition were determined for Hi-Nicalon and Hi-Nicalon S and compared that of Nicalon [31].

2. Experimental procedure

Two types of polycarbosilane-derived Si-C fibers, Hi-Nicalon and Hi-Nicalon S (Nippon Carbon Co., Tokyo, Japan), were employed in this study. Their composition and mean diameter are shown in Table I, along with those of Nicalon [32]. Nicalon contains a great amount of oxygen (11.7%) and an excess of carbon. Hi-Nicalon contains only a small amount of oxygen, though it contains a large excess of carbon. On the other hand, Hi-Nicalon S has a nearly stoichiometric composition. 500 mg of fibers, 30 mm in length were placed in a platinum crucible and then were oxidized

TABLE I Properties of polycarbosilane-derived SiC fibers [32]

	Nicalon	Hi-Nicalon	Hi-Nicalon S
Chemical composition			
Si (mass%)	56.6	62.4	68.9
C (mass%)	31.7	37.1	30.9
O (mass%)	11.7	0.5	0.2
C/Si atomic ratio	1.31	1.39	1.05
Fiber diameter (μm)	15	14	12
Density (kg/m^3)	2550	2740	3100

in an alumina tube of a vertical SiC resistance furnace for 72 ks (20 h) at 1773 K. Ar-O$_2$ gas mixture with oxygen partial pressures from 1 to 25000 Pa was allowed to flow into the alumina tube at a flow rate of 8.33×10^{-6} m^3/s. During oxidation, the mass change of the fibers was determined by a digital-type automatic recording balance. Upon completion of the oxidation, the fibers were cooled rapidly by raising the crucible to the low temperature zone of the furnace.

The oxidized fibers were subjected to X-ray diffraction analysis, resistivity measurement, SEM observation and tensile tests. Resistivity measurements and tensile tests were conducted for the fibers from which the silica film was removed with NH$_4$F + HF solution. Specific resistivity measurements were made at room-temperature, by applying direct current. Both ends of a fiber were attached with electron-conductive resin to copper electrode plates spaced 0.8 mm apart. Twenty measurements were made for each oxidized fiber. The room-temperature tensile strength of a fiber of 10 mm length was determined using a universal tensile tester (Orientec Co., Type TENSILON UTM-II-20. Tokyo, Japan) with a load cell of 4.9 N and a crosshead speed of 2 mm/min. The mean value for 20 measurements was taken as the tensile strength of each fiber.

3. Results
3.1. TG curves
Figs 1 and 2 show the TG curves for Hi-Nicalon and Hi-Nicalon S fibers oxidized at 1773 K under Ar-O$_2$ gas mixtures with different oxygen partial pressures (p_{O_2}).
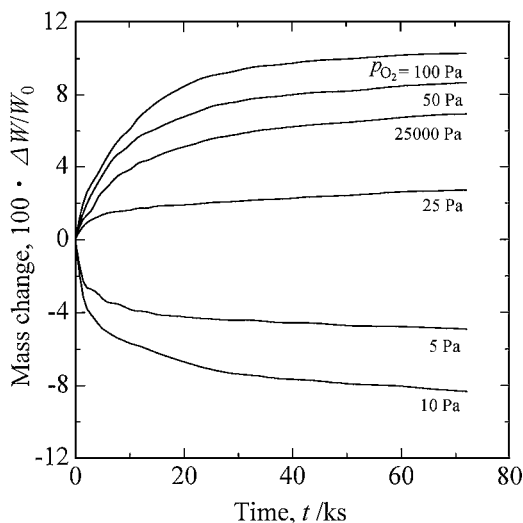
Figure 1 TG curves for Hi-Nicalon fibers heated at 1773 K in Ar-O$_2$ gas mixtures with different oxygen partial pressures.
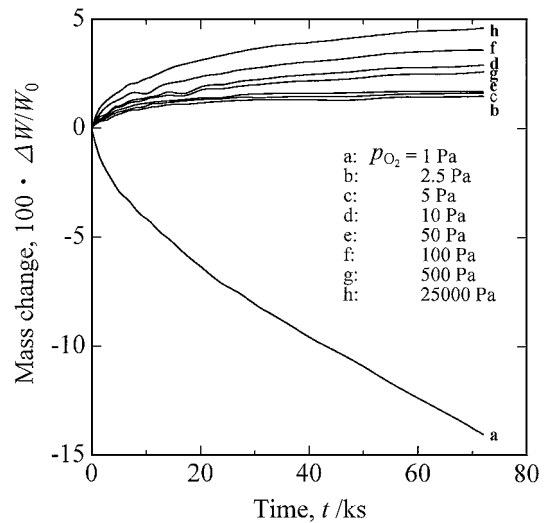
Figure 2 TG curves for Hi-Nicalon S fibers heated at 1773 K in Ar-O$_2$ gas mixtures with different oxygen partial pressures.

TG curves for Hi-Nicalon fibers are classified on the basis of mass gain at $p_{O_2} \geqq 25$ Pa and mass loss at $p_{O_2} \leqq 10$ Pa. For Hi-Nicalon S fibers, the change from the mass gain to mass loss regimes are observed for lower oxygen partial pressures ($p_{O_2} = 1$ Pa–2.5 Pa). The TG curve is intricately dependent upon the oxygen partial pressure in the range over which it exhibits a mass gain. While the mass gain is attributed to the passive-oxidation of SiC crystallites, the mass loss is attributed to the thermal decomposition of the amorphous silicon oxycarbide (SiC$_X$O$_Y$) phase, the oxidation of the free carbon phase or/and the subsequent active-oxidation of SiC crystallites. A retardation of passive-oxidation with decreasing the oxygen partial pressure can be expected. Therefore, it is noteworthy that the passive-oxidation of both fibers was enhanced by further decrease at $p_{O_2} \leqq 100$ Pa. A similar result was observed in the passive oxidation of Nicalon [31].

3.2. XRD analysis
XRD patterns for Hi-Nicalon and Hi-Nicalon S after 72 ks of oxidation at 1773 K and $p_{O_2} = 1$–100000 Pa are shown in Figs 3 and 4, respectively. The oxidation-treatments at $p_{O_2} \geqq 25$ Pa produced cristobalite phase
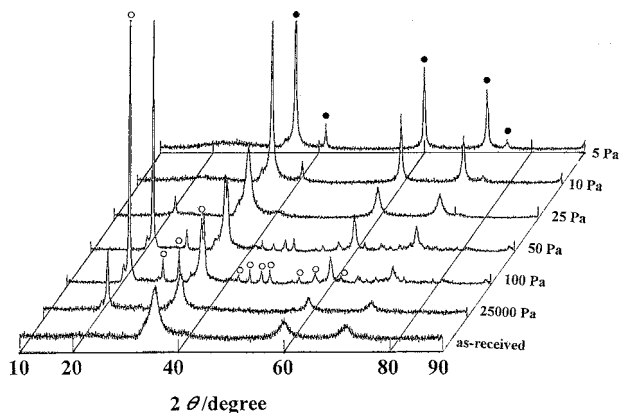
Figure 3 X-ray diffraction patterns for Hi-Nicalon fibers heated for 72 ks at 1773 K in Ar-O$_2$ gas mixtures with different oxygen partial pressures. ○ cristobalite, ● SiC.
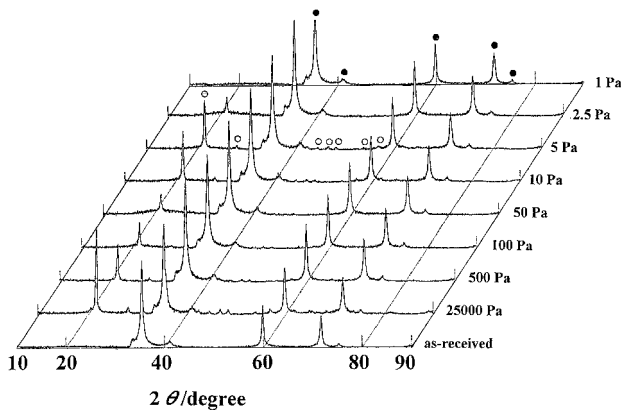
Figure 4 X-ray diffraction patterns for Hi-Nicalon S fibers heated for 72 ks at 1773 K in Ar-O_2 gas mixtures with different oxygen partial pressures. ○ cristobalite, ● SiC.
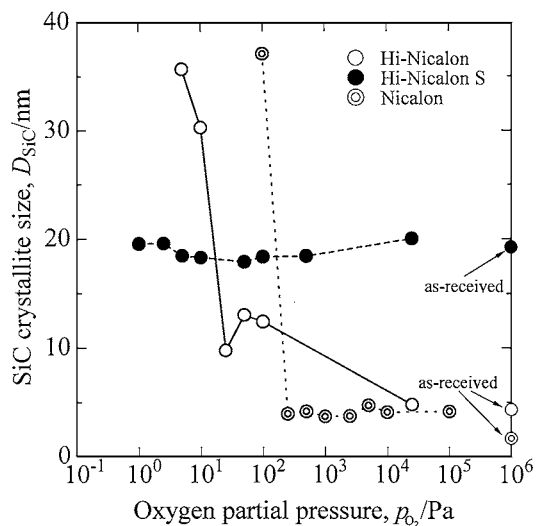

Figure 5 β-SiC crystallite size of fibers heated for 72 ks at 1773 K in Ar-O_2 gas mixtures with different oxygen partial pressures.

Figure 6 Specific resistivity of fibers heated for 72 ks at 1773 K in Ar-O_2 gas mixtures with different oxygen partial pressures.

3.3. Specific resistivity

Fig. 6 shows the relationship between the specific resistivity of the oxidized fibers and oxygen partial pressure. There is a 3-orders-of-magnitude drop in the resistivity of Nicalon after oxidation at $p_{O_2} = 100000$ Pa and $T = 1773$ K. A drop of resistivity was observed at oxygen partial pressure ranging from 100000 to 250 Pa, being followed by a marked increase of specific resistivity when p_{O_2} is lowered from 250 Pa to 100 Pa. The behavior of Hi-Nicalon was similar to that of Nicalon, though the resistivity varied only in the limited range of 0.01 to 0.1 Ωm. The thermal decomposition of SiC_XO_Y phase is responsible for the resistivity drop in the passive-oxidation region: at $p_{O_2} \geqq 250$ Pa for Nicalon and $p_{O_2} \geqq 25$ Pa for Hi-Nicalon. The resistivities of Nicalon and Hi-Nicalon fibers in the active-oxidation region were raised by four-orders-of-magnitude and by one-order-of-magnitude, respectively. On the other hand, the resistivity of Hi-Nicalon S is independent of p_{O_2} in the passive-oxidation region (at $p_{O_2} \geqq 2.5$ Pa), though it is one-order-of-magnitude higher than the resistivity in the as-received state. One-order-of-magnitude increase of resistivity was observed in the active-oxidation region (at $p_{O_2} = 1$ Pa).

3.4. Morphology of oxidized fibers

Fig. 7 shows SEM photographs of Hi-Nicalon fibers oxidized for 72 ks at 1773 K. After oxidation in the passive-oxidation region ($p_{O_2} = 50$ and 100 Pa), the fibers were coated with a thick film which was soluble in $NH_4F + HF$ solution (Photos A–D). XRD analysis shows that this film consists of cristobalite. The cristobalite film was smooth and pore-free, though cracked, due to the volume shrinkage associated with the cristobalite $\beta \to \alpha$ transition during cooling. The unoxidized cores display a glassy fractured surface and fine-grained structure, because of the suppression effect of the SiO_2 film on the thermal decomposition of the SiC_XO_Y phase (B, D). In particular, it may be noted that the unoxidized core is coated with a double layer in the fibers oxidized at $p_{O_2} = 50$ Pa (D). The fibers actively-oxidized

in Hi-Nicalon fibers. Particularly noteworthy is the very strong cristoballite peak in the fibers heat-treated at $p_{O_2} = 50$ and 100 Pa. The heat-treatment at $p_{O_2} \leqq 10$ Pa resulted in the disappearance of cristobalite and the appreciable growth of β-SiC. On the other hand, the XRD patterns of Hi-Nicalon S fibers display cristobalite peaks even after oxidation at $p_{O_2} = 2.5$ Pa. However, the cristobalite phase disappeared at $p_{O_2} = 1$ Pa. The disappearance of cristobalite at very low oxygen partial pressures implies the occurrence of active-oxidation. Thus, XRD results show a good consistency with TG data (Figs 1 and 2), revealing the active-to-passive oxidation transition at a p_{O_2} value between 10 and 25 Pa for Hi-Nicalon and at a p_{O_2} value between 1 and 2.5 Pa for Hi-Nicalon S.

Fig. 5 shows the β-SiC crystallite size of the fibers oxidized at $p_{O_2} = 1$–100000 Pa. The β-SiC crystallites in Hi-Nicalon fibers grew slightly in the passive-oxidation region and coarsened markedly in the active-oxidation region, as well as previously reported for Nicalon fibers [31]. On the other hand, the SiC crystallite size of Hi-Nicalon S fibers remained nearly identical to the size of about 20 nm in the as-received fibers throughout the passive- and active-oxidation region.
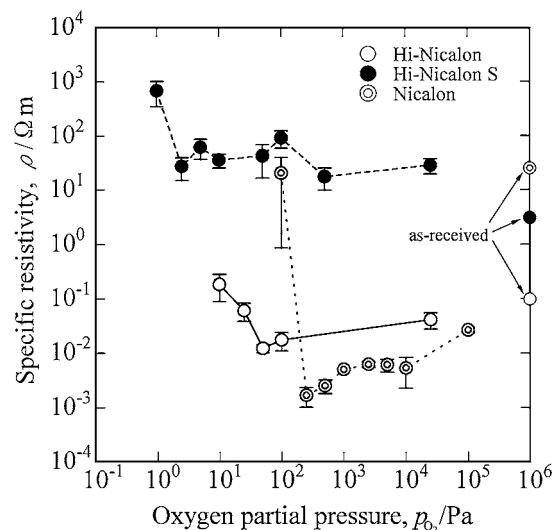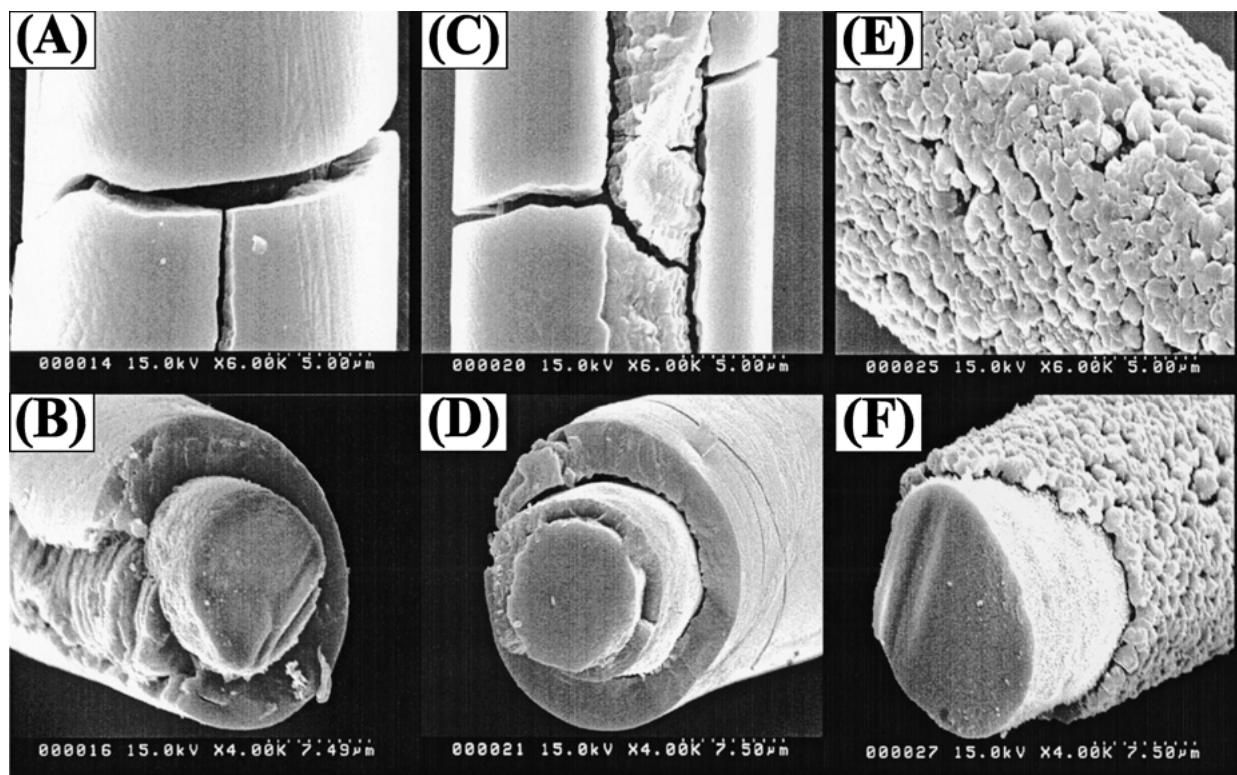
Figure 7 SEM photographs of Hi-Nicalon fibers heated for 72 ks in Ar-O$_2$ gas mixtures with oxygen partial pressures of 100 Pa (A, B), 50 Pa (C, D) and 10 Pa (E, F).

at $p_{O_2} = 10$ Pa exhibit a dual structure, showing that the active-oxidation took place towards the center of fibers. Hi-Nicalon has a coarse-grained surface as well as previously reported for Nicalon [31]; though it has a glassy core (E, F). Since XRD analysis shows the absence of SiO$_2$ film and the grain growth of β-SiC, the coarse grains observed on the fiber surface are β-SiC crystals.

Fig. 8 shows SEM photographs of Hi-Nicalon S fibers oxidized for 72 ks at 1773 K. The fibers oxidized at a high oxygen pressure ($p_{O_2} = 25000$ Pa) are coated with a thick and cracked cristobalite film (A, B).
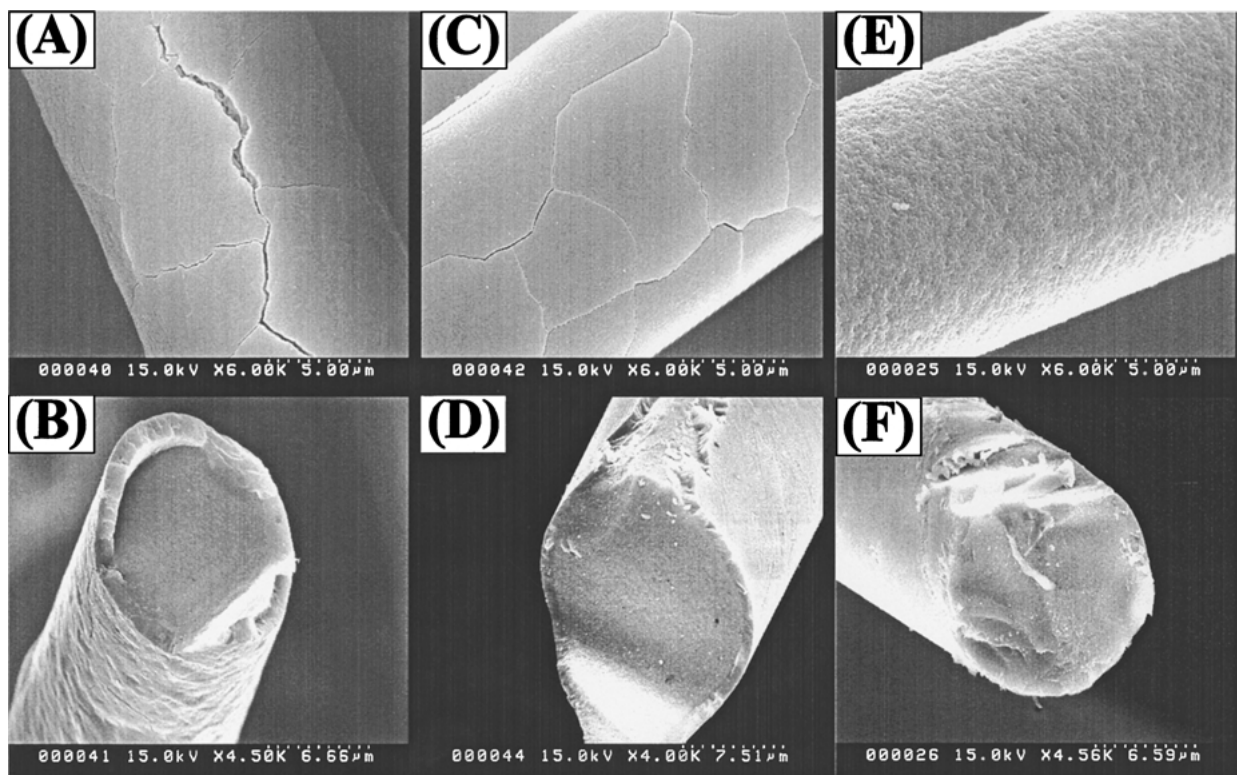

Figure 8 SEM photographs of Hi-Nicalon S fibers heated for 72 ks in Ar-O$_2$ gas mixtures with oxygen partial pressures of 25000 Pa (A, B), 5 Pa (C, D) and 1 Pa (E, F).
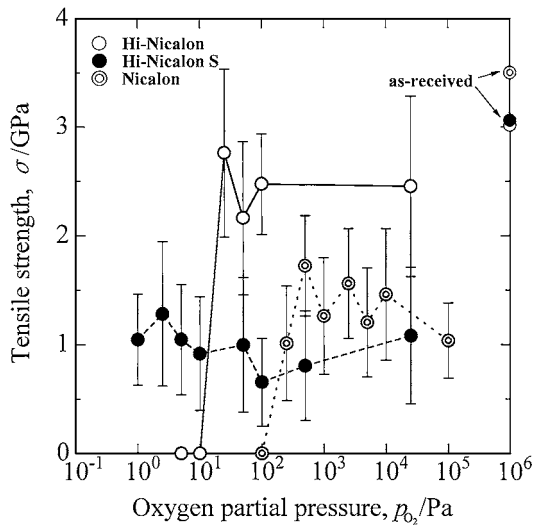
Figure 9 Tensile strength of fibers heated for 72 ks at 1773 K in Ar-O_2 gas mixtures with different oxygen partial pressures.

A thin cristobalite film was observed even at $p_{O_2} = 5\,\text{Pa}$ (C, D). Hi-Nicalon S oxidized in the active-oxidation region (at $p_{O_2} = 1\,\text{Pa}$) also display a dual structure, though the surface layer is a fine-grained and pore-free (E and F).
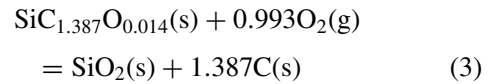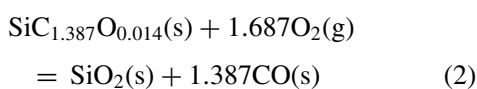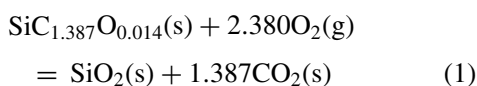
3.5. Tensile strength

Fig. 9 shows the residual room-temperature strength of oxidized fibers as a function of oxygen partial pressure during the oxidation tests. The strength of Nicalon fibers also are shown [31]. Tensile tests were conducted on fibers after having removed the SiO_2 film (unoxidized cores). While the passive-oxidation caused a marked degradation of strength for both Nicalon and Hi-Nicalon S fibers, it only caused a slight degradation of strength for Hi-Nicalon fibers. In addition, the tensile strength for three types of fibers were practically independent of the oxygen partial pressures in the passive-oxidation region. On being actively oxidized, both Nicalon and Hi-Nicalon fibers were too fragile to be submitted to a tensile test. On the other hand, it may be noted that the strength of Hi-Nicalon S fibers has a nearly identical value throughout oxygen partial pressures from passive-oxidation to active-oxidation region (about 1 GPa).
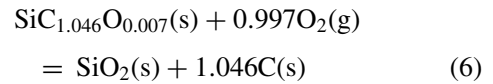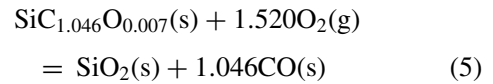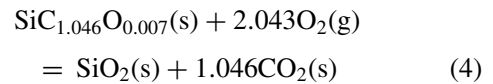
4. Discussion

Hi-Nicalon and Hi-Nicalon S fibers, as well as Nicalon fibers, may be oxidized passively or actively, depending on the oxygen partial pressures. The overall reactions for the passive-oxidation which yields a mass gain are represented as follows, on the basis of their actual chemical composition:
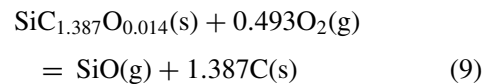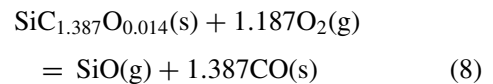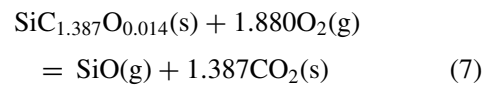for Hi-Nicalon:

$$SiC_{1.387}O_{0.014}(s) + 2.380O_2(g)$$
$$= SiO_2(s) + 1.387CO_2(s) \qquad (1)$$

$$SiC_{1.387}O_{0.014}(s) + 1.687O_2(g)$$
$$= SiO_2(s) + 1.387CO(s) \qquad (2)$$

$$SiC_{1.387}O_{0.014}(s) + 0.993O_2(g)$$
$$= SiO_2(s) + 1.387C(s) \qquad (3)$$

for H-Nicalon S:

$$SiC_{1.046}O_{0.007}(s) + 2.043O_2(g)$$
$$= SiO_2(s) + 1.046CO_2(s) \qquad (4)$$

$$SiC_{1.046}O_{0.007}(s) + 1.520O_2(g)$$
$$= SiO_2(s) + 1.046CO(s) \qquad (5)$$

$$SiC_{1.046}O_{0.007}(s) + 0.997O_2(g)$$
$$= SiO_2(s) + 1.046C(s) \qquad (6)$$

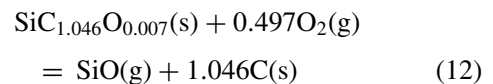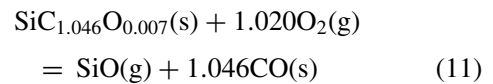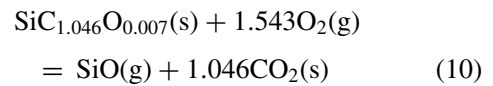On the other hand, the active-oxidation results in a serious mass loss according to the following overall reactions:
for Hi-Nicalon:

$$SiC_{1.387}O_{0.014}(s) + 1.880O_2(g)$$
$$= SiO(g) + 1.387CO_2(s) \qquad (7)$$

$$SiC_{1.387}O_{0.014}(s) + 1.187O_2(g)$$
$$= SiO(g) + 1.387CO(s) \qquad (8)$$

$$SiC_{1.387}O_{0.014}(s) + 0.493O_2(g)$$
$$= SiO(g) + 1.387C(s) \qquad (9)$$

for H-Nicalon S:

$$SiC_{1.046}O_{0.007}(s) + 1.543O_2(g)$$
$$= SiO(g) + 1.046CO_2(s) \qquad (10)$$

$$SiC_{1.046}O_{0.007}(s) + 1.020O_2(g)$$
$$= SiO(g) + 1.046CO(s) \qquad (11)$$

$$SiC_{1.046}O_{0.007}(s) + 0.497O_2(g)$$
$$= SiO(g) + 1.046C(s) \qquad (12)$$

Which type of reaction actually takes place is strongly dependent upon the oxygen partial pressure.

Fig. 10 shows the mass change of the fibers oxidized for 72 ks as a function of the oxygen partial pressure, p_{O_2}. For comparison, the results for Nicalon fibers are also shown [31]. Mass gains were observed at $p_{O_2} \geq 25\,\text{Pa}$ for Hi-Nicalon, at $p_{O_2} \geq 2.5\,\text{Pa}$ for Hi-Nicalon S and at $p_{O_2} \geq 250\,\text{Pa}$ for Nicalon, providing proof that the fibers were subjected to passive-oxidation. The occurrence of passive-oxidation is verified by the formation of cristobalite film (Figs 3, 4, 7 and 8). The fact that the mass gain decreases with a decrease in oxygen partial pressure at $p_{O_2} \geq 1000\,\text{Pa}$ will usually be found reasonable. It is noteworthy that an increase of mass gain was observed in the oxygen partial pressure range from 1000 to 10 Pa. This implies a change in the reaction mechanism of passive-oxidation. With decrease in oxygen partial pressure, the passive-oxidation may change in this order: reaction (1)–(3) for Hi-Nicalon fibers and reaction (4)–(6) for Hi-Nicalon S fibers, respectively. AES analysis of Nicalon fibers
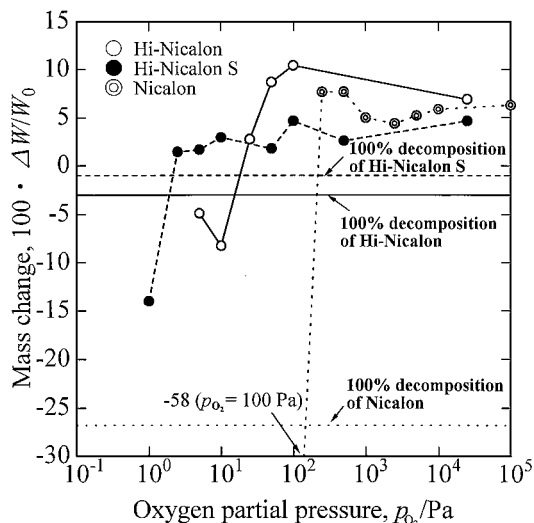
Figure 10 Mass change of fibers heated for 72 ks at 1773 K in Ar-O_2 gas mixtures with different oxygen partial pressures.

oxidized at $p_{O_2} = 500$ Pa shows the formation of an intermediate carbon layer between the SiO_2 film and the unoxidized core [31]. For Hi-Nicalon fibers oxidized at $p_{O_2} = 50$ Pa, the unoxidized core was coated with a double layer: a cristobalite layer and probably a carbon-enriched layer (Fig. 7, D). This is because a concentration gradient of oxygen gas is formed across the SiO_2 film and the oxygen partial pressure at the SiO_2 film-unoxidized interface is low enough to allow reactions (3) and (6) to occur. The reactions enhance the mass gain, owing to the absence of the formation of gaseous products. Thus, the passive-oxidation at $p_{O_2} = 10$–1000 Pa produces a maximum in the relationship between the mass gain and p_{O_2}.

On the other hand, at $p_{O_2} \leqq 10$ Pa for Hi-Nicalon and at $p_{O_2} \leqq 1$ Pa for Hi-Nicalon S, there was a relatively large loss of mass and cristobalite was not detected (Figs 1–4). In addition, the β-SiC grain structures of the fiber surface were coarsened (Figs 7 and 8). These results suggest that the thermal decomposition of the amorphous silicon oxycarbide (SiC_XO_Y) phase and the subsequent active oxidation of SiC occurred. For Nicalon, the active-oxidation took place at $p_{O_2} = 100$ Pa [31]. Thus, the oxygen partial pressure for the active-to-passive oxidation transition is lowered by one-order-of-magnitude in the following order: Nicalon, Hi-Nicalon and Hi-Nicalon S. This is caused by the different compositions of fibers: the amount of amorphous silicon oxycarbide (SiC_XO_Y) and excess carbon. The thermal decomposition of SiC_XO_Y phase may take place at the experiment temperature (1773 K):

$$SiC_XO_Y(s) \rightarrow SiC(s) + SiO(g) + CO(g) \qquad (13)$$
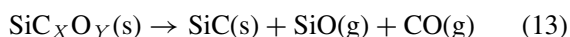
The SiC_XO_Y phase crystallizes into β-SiC, resulting in a mass loss associated with the generation of SiO and CO gases. Reaction (13) essentially takes place in any environments, causing the grain growth of β-SiC and the decrease in resistivity. As shown in Figs 5 and 6, the above reaction took place in Nicalon and Hi-Nicalon fibers. Since SiO_2 film may prevent the evolution of the decomposition gases in the passive-

oxidation range; the SiC_XO_Y phase was decomposed only at the earliest stage of oxidation [33]. On the other hand, for Hi-Nicalon S fibers, no grain growth of β-SiC and one-order-of-magnitude increase in resistivity were found because of a nearly stoichiometric composition (Figs 5 and 6). The increase in resistivity may be attributed to partial deconstruction of the conductive circuit by the oxidation. This appears to be because oxygen molecules penetrate into grain boundaries and oxidize the surface around SiC grains. When oxidized in the active oxidation region, there was a significant increase in resistivity over the as-received values. The active-oxidation causes a marked increase in the porosity of fiber structure, offering any hindrance to the electrical conduction of the fibers (Fig. 6).

The maximum mass losses after high-temperature exposure in argon (100% decomposition of SiC_XO_Y phase) were 26% for Nicalon, 3% for Hi-Nicalon and 1% for Hi-Nicalon S. All the mass loss after oxidation at $p_{O_2} = 100$ Pa for Nicalon [31], $p_{O_2} = 5$ and 10 Pa for Hi-Nicalon and $p_{O_2} = 1$ Pa for Hi-Nicalon S exceed the above values of 100% decomposition for each fiber, respectively. This shows that the thermal decomposition of SiC_XO_Y phase was followed by the active-oxidation of β-SiC crystallites in Ar-O_2 gas. The thermal decomposition may be regarded as the active-oxidation by the oxygen from SiC_XO_Y phase. After the oxygen in SiC_XO_Y phase is consumed by the thermal decomposition, the β-SiC crystals as a decomposition product are actively oxidized by O_2 gas. SEM observation shows that the active-oxidation initially takes place only at the surface of the fibers (Fig. 7, F). Subsequently the unoxidized core is reduced towards the center, leaving behind a porous and coarse-grained layer. Distinct dual structure was found in Nicalon and Hi-Nicalon fibers [31]. On the other hand, the active-oxidation of Hi-Nicalon S caused a slight coarsening of β-SiC crystals. As shown in Fig. 5, the SiC crystallite size was almost identical to the value (about 20 nm) in the as-received state throughout the passive-oxidation and active-oxidation region. This differing behavior can be probably attributed to a difference in microstructure of fibers. Nicalon and Hi-Nicalon consist of a fine-grained β-SiC (2 and 4 nm in size) which is embedded in the SiC_XO_Y phase and free carbon. The intergranular SiC_XO_Y and free carbon phases disappear as a result of thermal decomposition and active-oxidation. Consequently, the surface of a β-SiC crystal is allowed to come into contact with the newly formed surface of other crystals, causing the coalescence of fine β-SiC grains. On the other hand, for Hi-Nicalon S fibers with a stoichiometric composition, as a result of the absence of SiC_XO_Y and free carbon, β-SiC crystals are probably brought into direct contact with each other in the as-received state. Therefore, a temperature above 1773 K is probably required in order to yield the coalescence of SiC into larger grains owing to the small contact area between coarse grains.

Nicalon lost its strength after active-oxidation [31]. Hi-Nicalon also was seriously damaged by active-oxidation (Fig. 7), resulting in a resistivity increase and a marked strength degradation to 0 GPa (Figs 6 and 9). On the other hand, the tensile strength of Hi-Nicalon S
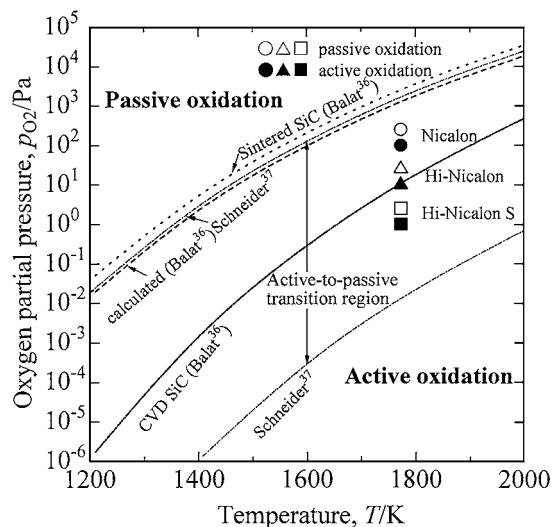
Figure 11 Oxygen partial pressure for active-to-passive oxidation transition of SiC as function of temperature.

was held at about 1 GPa throughout passive-oxidation and active-oxidation regions, though the resistivity increased by one-order-of-magnitude. This seems to be because the fiber surface was pore-free even after active-oxidation (Fig. 8).

The active-to-passive oxidation transition of silicon carbide has been investigated in terms of theoretical and experimental approaches. Fig. 11 shows typical temperature dependence of the oxygen partial pressure for the active-to-passive oxidation transition of silicon carbide [11, 12]. The active-to-passive transition is strongly affected by factors such as the type of silicon carbide, total gas pressure and gas flow rate, as well as temperature and oxygen partial pressure. To summarize the active-to-passive transition determined under different conditions, Schneider *et al.* indicate that the oxygen partial pressure for active-to-passive transition varies over 4–7 orders of magnitude. The active-to-passive transitions for three types of polycarbosilane-derived SiC fibers, Nicalon, Hi-Nicalon and Hi-Nicalon S, are within this transition region. The oxygen partial pressure of the active-to-passive transition is lowered by one-order-of-magnitude in the following order: $p_{O_2} = 100–250$ Pa for Nicalon, $p_{O_2} = 10–25$ Pa for Hi-Nicalon and $p_{O_2} = 1–2.5$ Pa for Hi-Nicalon S. This could be attributed to different contents of oxygen and excess carbon in the fibers, as shown in Table I. Oxygen is present as silicon oxycarbide (SiC_XO_Y) in the fibers. At the oxidation temperature (1773 K), the SiC_XO_Y phase crystallizes into β-SiC, generating SiO and CO. For Nicalon with high oxygen content (11.7 mass% O), as a consequence of vigorous generation of the decomposition gases, the oxygen partial pressure of the supplied gas (Ar-O₂ gas mixture) is lowered at the interstices between fibers. In addition, the CO generation by the selective oxidation of excess carbon also may contribute greatly to the lowering of oxygen partial pressure. As a result, Nicalon fibers are actively oxidized in Ar-O₂ gas mixture with an high oxygen partial pressure of 100 Pa. While Hi-Nicalon fibers have similar excess carbon, it is almost free from SiC_XO_Y phase. Therefore, the oxygen partial pressure for the active oxidation of Hi-Nicalon

fibers ($p_{O_2} = 10$ Pa) is one-order-of-magnitude lower than that for the active oxidation of Nicalon fibers ($p_{O_2} = 100$ Pa). The active-oxidation of Hi-Nicalon S fibers, which have a nearly stoichiometric composition, occurs at a still lower oxygen partial pressure ($p_{O_2} = 1$ Pa), owing to only slight gas generation.

5. Summary
Three types of polycarbosilane-derived SiC fibers were oxidized at 1773 K in Ar-O₂ gas mixtures with oxygen partial pressures from 1 to 100000 Pa to investigate the active-to-passive oxidation transition through TG, XRD analysis, SEM observation and tensile test. The steady mass gain and the formation of a pore-free cristobalite film were observed at $p_{O_2} \geqq 250$ Pa for Nicalon, $p_{O_2} \geqq 25$ Pa for Hi-Nicalon and $p_{O_2} \geqq 2.5$ Pa for Hi-Nicalon S, revealing the occurrence of passive-oxidation. In addition, 40–80% of initial strength was retained after passive-oxidation. On the other hand, the active-oxidation which is characterized by a mass loss and the absence of silica film occurred at $p_{O_2} \leqq 100$ Pa for Nicalon, $p_{O_2} \leqq 10$ Pa for Hi-Nicalon and $p_{O_2} \leqq 1$ Pa for Hi-Nicalon S. Although the fiber strength after active-oxidation was lost for Nicalon and Hi-Nicalon, 35% of initial strength was retained for Hi-Nicalon S (about 1 GPa). p_{O_2} values for active-to-passive oxidation transition are dependent upon the amounts of silicon oxycarbide and excess carbon in fibers.

Acknowledgement

References
1. D. E. ROSNER and H. D. ALLENDORF, *J. Phys. Chem.* **74** (1970) 1829.
2. E. A. GULBRANSEN and S. A. JANSSON, *Oxid. Met.* **4** (1972) 181.
3. S. C. SINGHAL, *Ceramurgia* **2** (1976) 123.
4. J. W. HINZE and H. C. GRAHAM, *J. Electrochem. Soc.* **123** (1976) 1066.
5. R. PAMPUCH and S. JONAS, *Sci. Ceram.* **9** (1977) 300.
6. L. VAUGHN and H. G. MAAHS, *J. Amer. Ceram. Soc.* **73** (1990) 1540.
7. A. H. HEIER and V. L. LOU, *ibid.* **73** (1990) 2789.
8. T. NARUSHIMA, T. GOTO, Y. IGUCHI and T. HIRAI, *ibid.* **74** (1991) 2583.
9. M. J. H. BALAT, G. FLAMANT, G. MALÉ and G. PICHELIN, *J. Mater. Sci.* **27** (1992) 697.
10. K. G. NICKEL, *J. Europ. Ceram. Soc.* **9** (1992) 3.
11. M. J. H. BALAT, *ibid.* **16** (1996) 55.
12. B. SCHNEIDER, A. GUETTE, R. NASLAIN, M. CATALDI and A. COSTECALDE, *J. Mater. Sci.* **33** (1998) 535.
13. Y. MANIETTE and A. OBERLIN, *ibid.* **24** (1989) 3361.
14. L. FILIPUZZI and R. NASLAIN, in Proc. 7th CIMTEC (Elsevier, Amsterdam, 1991) p. 35.
15. H. E. KIM and A. J. MOORHEAD, *J. Amer. Ceram. Soc.* **74** (1991) 666.
16. T. SHIMOO, H. CHEN and K. OKAMURA, *J. Ceram. Soc. Jpn* **100** (1992) 929.
17. T. SHIMOO, T. HAYATSU, M. TAKEDA, H. ICHIKAWA, T. SEGUCHI and K. OKAMURA, *ibid.* **102** (1994) 617.

18. M. H. BERGER, N. HOCHET and A. R. BUNSELL, *J. Microsc.* **177** (1995) 230.
19. P. LE. COUSTUMER, M. MONTHIOUX and A. OBERLIN, *Br. Ceram. Trans.* **94** (1995) 177.
20. G. CHOLLON, R. R. PAILLER, R. NASLAIN, F. LAANANI, M. MONTHIOUX and P. OLRY, *J. Mater. Sci.* **32** (1997) 327.
21. G. CHOLLON, M. CZEERNIAK, R. PAILLER, X. BOURRA, R. NASLAIN, J. P. PILLOT and R. CANNET, *ibid.* **32** (1997) 893.
22. M. H. BERGER, N. HOCHET and A. R. BUNSELL, *J. Microsc.* **185** (1997) 243.
23. T. SHIMOO, F. TOYODA and K. OKAMURA, *J. Ceram. Soc. Jpn* **106** (1998) 447.
24. Y. T. ZHU, S. T. TAYLOR, M. G. STOUT, D. P. BUTT and T. C. LOWE, *J. Amer. Ceram. Soc.* **81** (1998) 655.
25. T. SHIMOO, F. TOYODA and K. OKAMURA, *J. Ceram. Soc. Jpn* **107** (1999) 263.
26. M. TAKEDA, J. SAKAMOTO, Y. IMAI and H. ICHIKAWA, *Composites Sci. and Tech.* **59** (1999) 813.
27. T. SHIMOO, F. TOYODA and K. OKAMURA, *J. Mater. Sci.* **35** (2000) 3301.
28. *Idem., J. Amer. Ceram. Soc.* **83** (2000) 1450.
29. *Idem., J. Mater. Sci.* **35** (2000) 3811.
30. T. SHIMOO, H. TAKEUCHI, M. TAKEDA and K. OKAMURA, *J. Ceram. Soc. Jpn* **108** (2000) 1096.
31. T. SHIMOO, Y. MORISADA and K. OKAMURA, *J. Am. Ceram. Soc.* **83** (2000) 3049.
32. M. TAKEDA, J. SAKAMOTO, A. SAEKI, Y. IMAI and H. ICHIKAWA, *Ceram. Eng. Sci. Proc.* **19** (1995) 37.
33. T. SHIMOO, F. TOYODA and K. OKAMURA, *J. Ceram. Soc. Jpn* **107** (1999) 263.